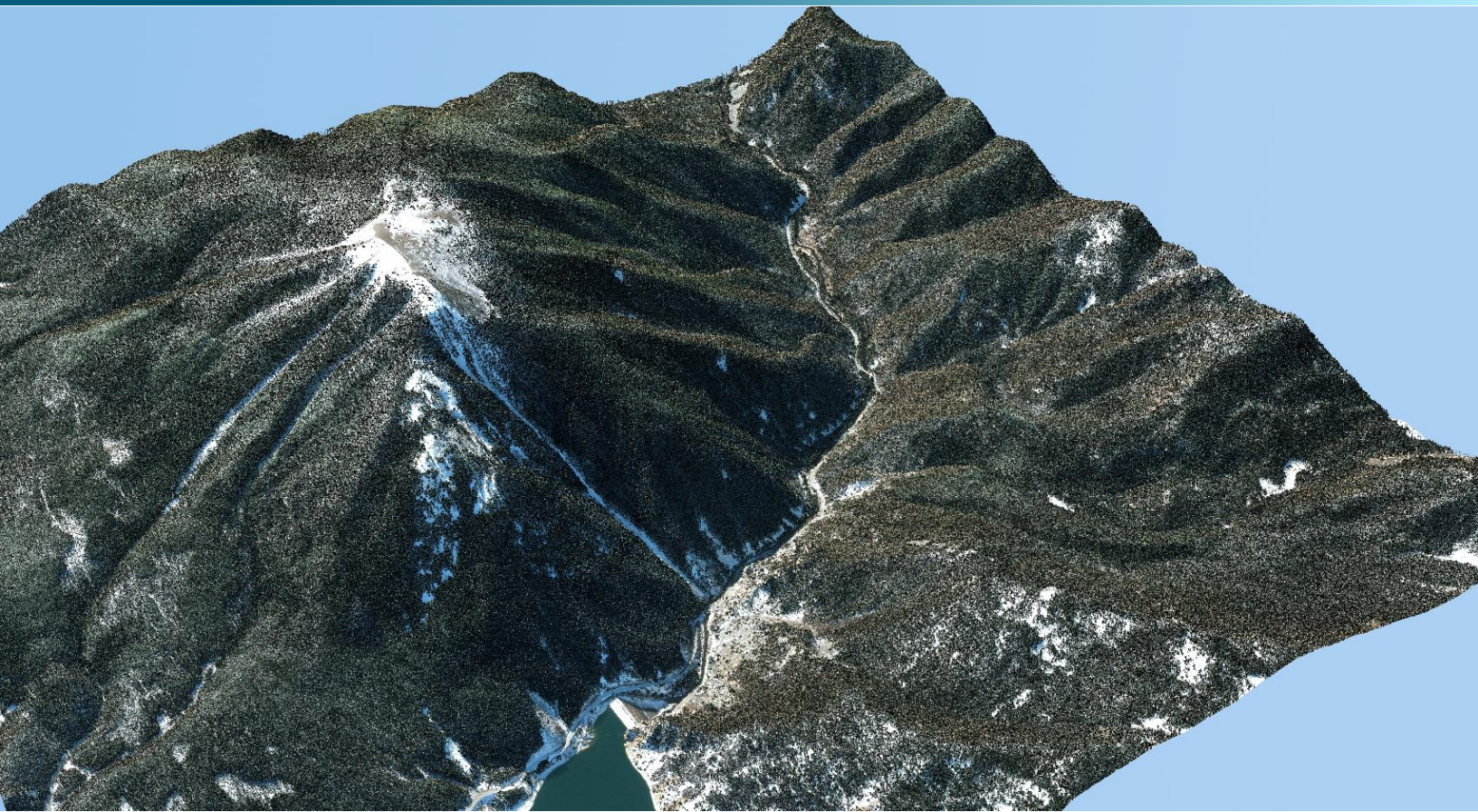


July 17, 2020



CWCB Montrose, Colorado Lidar

Technical Data Report

Prepared For:



COLORADO

Colorado Water
Conservation Board

Department of Natural Resources

Prepared By:



Marta Blanca Castano

Colorado Water Conservation Board

1313 Sherman Street, Rm. 718

Denver, CO 80203

PH: 303-866-3441 Ext.3230

QSI Corvallis

1100 NE Circle Blvd, Ste. 126

Corvallis, OR 97330

PH: 541-752-1204

TABLE OF CONTENTS

- INTRODUCTION 1
 - Deliverable Products 2
- ACQUISITION 4
 - Planning..... 4
 - Airborne Lidar Survey 5
 - Ground Survey..... 7
 - Base Stations..... 7
 - Ground Survey Points (GSPs)..... 9
 - Land Cover Class 10
- PROCESSING 12
 - Lidar Data 12
 - Feature Extraction 14
 - Hydroflattening and Water’s Edge Breaklines..... 14
 - Contours 15
- RESULTS & DISCUSSION..... 16
 - Lidar Density..... 16
 - Lidar Accuracy Assessments..... 20
 - Lidar Non-Vegetated Vertical Accuracy..... 20
 - Lidar Vegetated Vertical Accuracies 23
 - Lidar Relative Vertical Accuracy 24
 - Lidar Horizontal Accuracy 25
- CERTIFICATIONS 26
- GLOSSARY 27
- APPENDIX A - ACCURACY CONTROLS 28

Cover Photo: A view looking south-west across Taylor Park Reservoir, in the CWCB Montrose lidar project area. The image was created from the lidar bare earth model, overlaid with the 3D point cloud, and colored by NAIP imagery and elevation.

INTRODUCTION

This photo taken by QSI acquisition staff shows a view of the CWCB Montrose site in Colorado.



In June 2019, Quantum Spatial (QSI) was contracted by Department of Natural Resources Colorado Water Conservation Board (CWCB) to collect Light Detection and Ranging (lidar) data in the summer of 2019 for the CWCB Montrose site in Colorado. Data were collected to aid CWCB in assessing the topographic and geophysical properties of the study area to support FEMA flood modeling and mapping.

This report accompanies the delivered lidar data, and documents contract specifications, data acquisition procedures, processing methods, and analysis of the final dataset including lidar accuracy and density. Acquisition dates and acreage are shown in Table 1, a complete list of contracted deliverables provided to CWCB is shown in Table 2, and the project extent is shown in Figure 1.

Table 1: Acquisition dates, acreage, and data types collected on the CWCB Montrose site

Project Site	Contracted Acres	Buffered Acres	Acquisition Dates	Data Type
CWCB Montrose	2,637,770	2,657,120	08/21/2019-09/24/2019	lidar

Deliverable Products

Table 2: Products delivered to CWCB for the CWCB Montrose site

CWCB Montrose Lidar Products Projection: Albers Conformal Conic Horizontal Datum: NAD83 (2011) Vertical Datum: NAVD88 (GEOID12B) Units: Meters	
Points	LAS v 1.4 <ul style="list-style-type: none"> All Classified Returns
Rasters	1.0 Meter GeoTiffs <ul style="list-style-type: none"> DZ Orthos Hydroflattened Bare Earth Model (DEM)
Vectors	Indices Geodatabase (*.gdb) <ul style="list-style-type: none"> Contracted Project Boundary Buffered Project Boundary Delivery Blocks Boundaries Lidar Tile Index Contours (*.gdb) <ul style="list-style-type: none"> Topographic Contours (0.5 meter) Flightline Shapes Geodatabase (*.gdb) <ul style="list-style-type: none"> Flightline Index Flightline Swaths Ground Survey Shapes Geodatabase (*.gdb) <ul style="list-style-type: none"> Ground Control Points Non Vegetated Vertical Accuracy Check Points Vegetated Vertical Accuracy Check Points Monuments Ground Survey Shapes (.CSV) <ul style="list-style-type: none"> Ground Control Points Non Vegetated Vertical Accuracy Check Points Vegetated Vertical Accuracy Check Points Monuments Breakline Geodatabase (*.gdb) <ul style="list-style-type: none"> Water's Edge Breaklines Bridge Breaklines

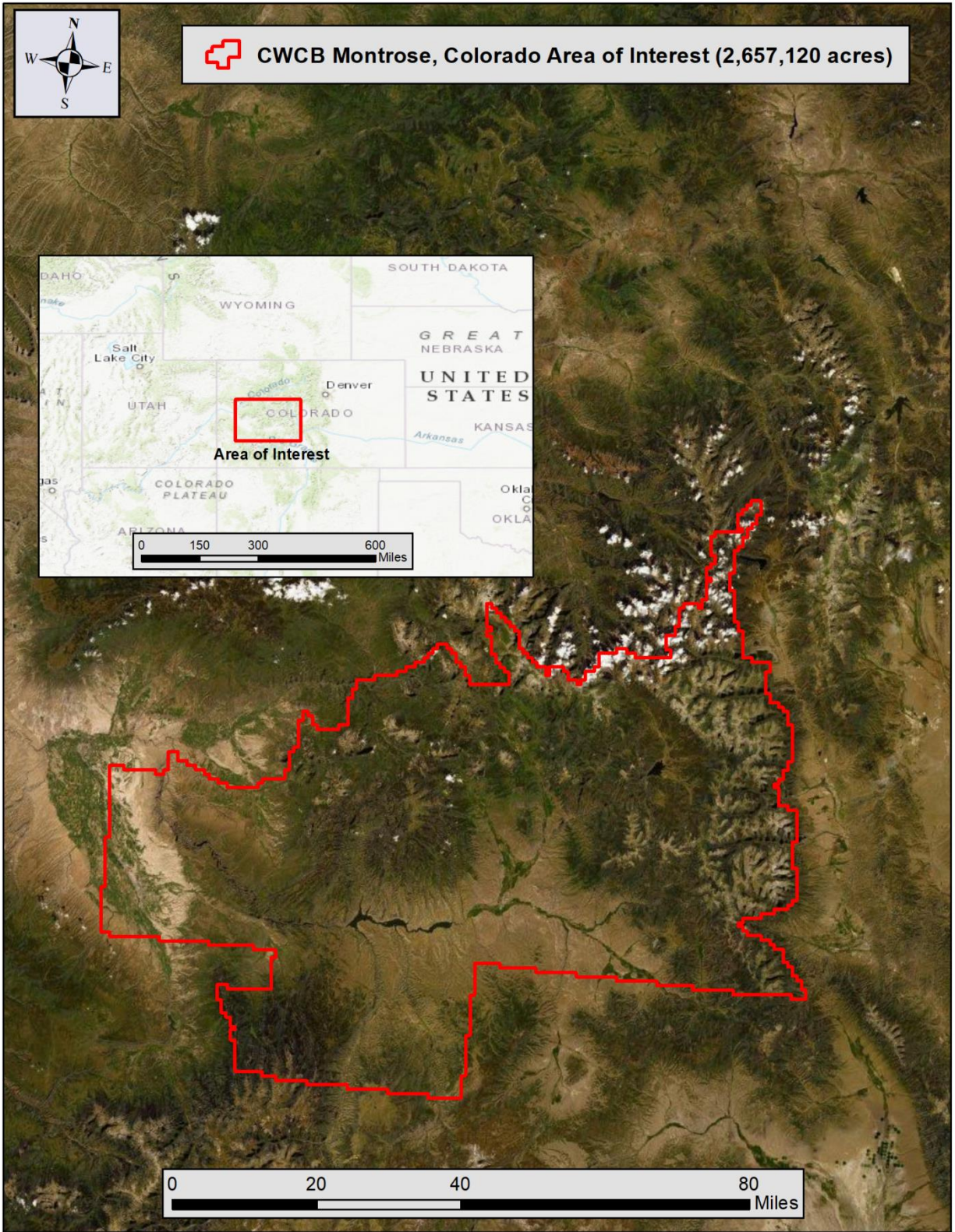


Figure 1: Location map of the CWCB Montrose site in Colorado

QSI's Cessna Caravan



Planning

In preparation for data collection, QSI reviewed the project area and developed a specialized flight plan to ensure complete coverage of the CWCB Montrose lidar study area at the target point density of ≥ 2.0 points/m². Acquisition parameters including orientation relative to terrain, flight altitude, pulse rate, scan angle, and ground speed were adapted to optimize flight paths and flight times while meeting all contract specifications.

Factors such as satellite constellation availability and weather windows must be considered during the planning stage. Any weather hazards or conditions affecting the flight were continuously monitored due to their potential impact on the daily success of airborne and ground operations. Logistical considerations including private property access and potential air space restrictions were reviewed. In addition, data collection was scheduled around leaf-off conditions to ensure complete collection.

Airborne Lidar Survey

The lidar survey was accomplished using a Riegl VQ1560i system mounted in a Cessna Caravan. Table 3 summarizes the settings used to yield an average pulse density of ≥ 2 pulses/m² over the CWCB Montrose project area. The Riegl laser system can record unlimited range measurements (returns) per pulse. It is not uncommon for some types of surfaces (e.g., dense vegetation or water) to return fewer pulses to the lidar sensor than the laser originally emitted. The discrepancy between first return and overall delivered density will vary depending on terrain, land cover, and the prevalence of water bodies. All discernible laser returns were processed for the output dataset.

Table 3: Lidar specifications and survey settings

Lidar Survey Settings & Specifications	
Acquisition Dates	August 21 – September 24, 2019
Aircraft Used	Cessna Caravan
Sensor	Riegl
Laser	VQ1560i
Maximum Returns	15
Resolution/Density	Average 2 pulses/m ²
Nominal Pulse Spacing	0.70 m
Survey Altitude (AGL)	1,159 m
Survey speed	135 knots
Field of View	58.5°
Mirror Scan Rate	23.2 Lines Per Second Per Scanner
Target Pulse Rate	350 kHz
Pulse Length	3 ns
Laser Pulse Footprint Diameter	21 cm
Central Wavelength	1064 nm
Pulse Mode	Uniform Point Spacing
Beam Divergence	0.18 mrad
Swath Width	2,582 m
Swath Overlap	20 %
Intensity	16-bit
Accuracy	NVA (95% Confidence Level) ≤ 10 cm
	VVA (95 th Percentile) ≤ 30 cm



Leica VQ1560i lidar sensor

All areas were surveyed with an opposing flight line side-lap of $\geq 20\%$ ($\geq 40\%$ overlap) in order to reduce laser shadowing and increase surface laser painting. To accurately solve for laser point position (geographic coordinates x, y and z), the positional coordinates of the airborne sensor and the attitude of the aircraft were recorded continuously throughout the lidar data collection mission. Position of the aircraft was measured twice per second (2 Hz) by an onboard differential GPS unit, and aircraft attitude was measured 200 times per second (200 Hz) as pitch, roll and yaw (heading) from an onboard inertial measurement unit (IMU). To allow for post-processing correction and calibration, aircraft and sensor position and attitude data are indexed by GPS time.



QSI's ground survey equipment in the CWCB Montrose project boundary.

Ground Survey

Ground control surveys, including monumentation and ground survey points (GSPs) were conducted to support the airborne acquisition. Ground control data were used to geospatially correct the aircraft positional coordinate data and to perform quality assurance checks on final lidar data.



QSI-Established Monument

Base Stations

Base stations were utilized for collection of ground survey points using real time kinematic (RTK) and fast static (FS) survey techniques. RTK positioning is a relative-positioning method that improves the accuracy of GPS signals, which enhances the precision of location data obtained from satellite-based systems; because RTK positioning allows one to obtain centimeter-level positioning in real time, it remains the procedure of choice for applications that demand high-precision mapping.

Monument locations were selected with consideration for satellite visibility, field crew safety, and optimal location for GSP coverage. QSI established eleven new monument and utilized five permanent active CORS stations for the CWCB Montrose Lidar project (Table 4, Figure 2). New monuments were established with a 6 to 8 inch MagHub spike and hard plastic reference washer. QSI's professional land surveyor, Steven J. Hyde (COPLS#38558) oversaw and certified the establishment and occupation of all monuments.

Table 4: Monument positions for the CWCB Montrose acquisition. Coordinates are on the NAD83 (2011) datum, epoch 2010.00

Monument ID	Latitude	Longitude	Ellipsoid (meters)
CWCB_01	39° 14' 54.80354"	-106° 28' 10.76306"	3276.677
CWCB_02	39° 04' 44.39663"	-106° 31' 55.51834"	3155.949
CWCB_03	38° 29' 40.76291"	-106° 19' 32.83922"	3425.016
CWCB_04	38° 49' 39.26487"	-106° 24' 33.13859"	3681.676
CWCB_05	38° 39' 06.11417"	-106° 28' 11.17120"	3049.464
CWCB_06	38° 13' 19.06550"	-107° 31' 44.38461"	2774.146
CWCB_07	38° 30' 34.28869"	-106° 46' 45.57029"	2393.927
CWCB_11	38° 23' 30.47935"	-107° 26' 40.39332"	2571.295
CWCB_12	38° 16' 22.13371"	-107° 10' 15.06354"	2778.026
CWCB_13	38° 29' 12.14581"	-107° 24' 56.41205"	2394.923
CWCB_14	38° 33' 31.26193"	-107° 09' 15.63805"	2930.072
MC05	38° 44' 22.38389"	-108° 04' 22.68376"	1505.884
MC10	38° 27' 20.13732"	-107° 52' 42.39390"	1809.443
R301	38° 39' 23.73974"	-107° 35' 27.36713"	2024.999

Monument ID	Latitude	Longitude	Ellipsoid (meters)
TC01	37° 56' 16.90458"	-107° 48' 47.94594"	2678.325
TOCB	38° 52' 15.28872"	-106° 58' 55.31892"	2709.019

QSI utilized static Global Navigation Satellite System (GNSS) data collected at 1 Hz recording frequency for each base station. During post-processing, the static GNSS data were triangulated with nearby Continuously Operating Reference Stations (CORS) using the Online Positioning User Service (OPUS¹) for precise positioning. Multiple independent sessions over the same monument were processed to confirm antenna height measurements and to refine position accuracy.

Monuments were established according to the national standard for geodetic control networks, as specified in the Federal Geographic Data Committee (FGDC) Geospatial Positioning Accuracy Standards for geodetic networks.² This standard provides guidelines for classification of monument quality at the 95% confidence interval as a basis for comparing the quality of one control network to another. The monument rating for this project is shown in Table 5.

Table 5: Federal Geographic Data Committee monument rating for network accuracy

Direction	Rating
1.96 * St Dev _{NE} :	0.050 m
1.96 * St Dev _Z :	0.050 m

For the CWCB Montrose lidar project, the monument coordinates contributed no more than 5.6 cm of positional error to the geolocation of the final ground survey points and lidar, with 95% confidence.

¹ OPUS is a free service provided by the National Geodetic Survey to process corrected monument positions. <http://www.ngs.noaa.gov/OPUS>.

² Federal Geographic Data Committee, Geospatial Positioning Accuracy Standards (FGDC-STD-007.2-1998). Part 2: Standards for Geodetic Networks, Table 2.1, page 2-3. <http://www.fgdc.gov/standards/projects/FGDC-standards-projects/accuracy/part2/chapter2>

Ground Survey Points (GSPs)

Ground survey points were collected using real time kinematic (RTK) and fast-static (FS) survey techniques (Table 6). For RTK surveys, a roving receiver receives corrections from a nearby base station or Real-Time Network (RTN) via radio or cellular network, enabling rapid collection of points with relative errors less than 1.5 cm horizontal and 2.0 cm vertical. FS surveys compute these corrections during post-processing to achieve comparable accuracy. RTK surveys record data while stationary for at least five seconds, calculating the position using at least three one-second epochs. FS surveys record observations for up to fifteen minutes on each GSP in order to support longer baselines. All GSP measurements were made during periods with a Position Dilution of Precision (PDOP) of ≤ 3.0 with at least six satellites in view of the stationary and roving receivers. See Table 6 for Trimble unit specifications.

GSPs were collected in areas where good satellite visibility was achieved on paved roads and other hard surfaces such as gravel or packed dirt roads. GSP measurements were not taken on highly reflective surfaces such as center line stripes or lane markings on roads due to the increased noise seen in the laser returns over these surfaces. GSPs were collected within as many flightlines as possible; however, the distribution of GSPs depended on ground access constraints and monument locations and may not be equitably distributed throughout the study area (Figure 2).

Table 6: QSI ground survey equipment identification

Receiver Model	Antenna	OPUS Antenna ID	Use
Trimble R8	Integrated Antenna	TRM_R8_GNSS	Rover
Trimble R10	Integrated Antenna	TRMR10	Static

Land Cover Class

In addition to ground survey points, land cover class check points were collected throughout the study area to evaluate vertical accuracy. Vertical accuracy statistics were calculated for all land cover types to assess confidence in the lidar derived ground models across land cover classes (Table 7, see Lidar Accuracy Assessments, page 20).

Table 7: Land Cover Types and Descriptions

Land cover type	Land cover code	Example	Description	Accuracy Assessment Type
Short Grass	SH_GRASS		Maintained or low growth herbaceous grasslands	VVA
Tall Grass	TALL_GRASS		Herbaceous grasslands in advanced stages of growth	VVA
Forested	FR		Forested areas dominated by coniferous or deciduous species	VVA
Bare Earth	BARE, BE		Areas of bare earth surface	NVA
Urban	URBAN		Areas dominated by urban development, including parks	NVA

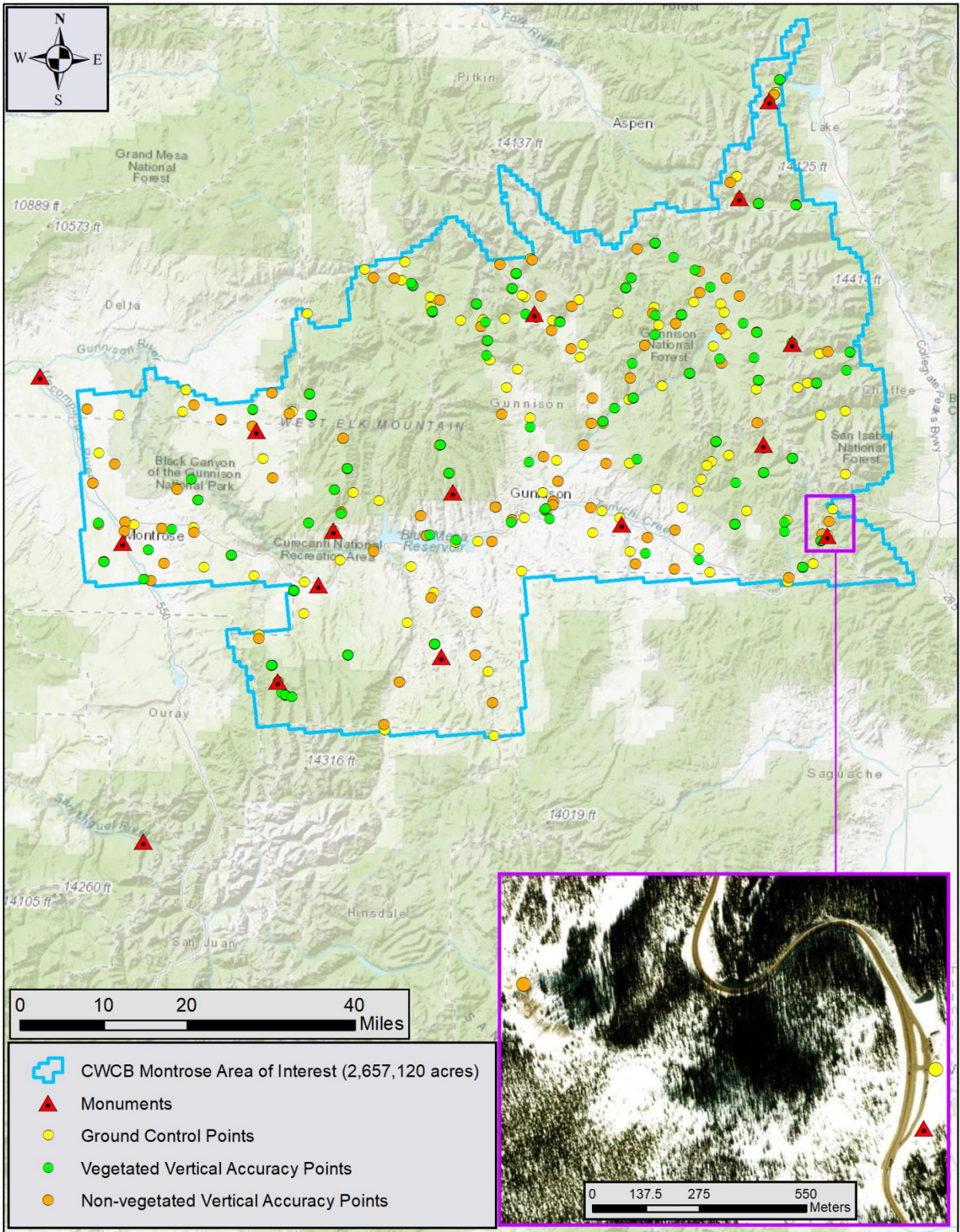
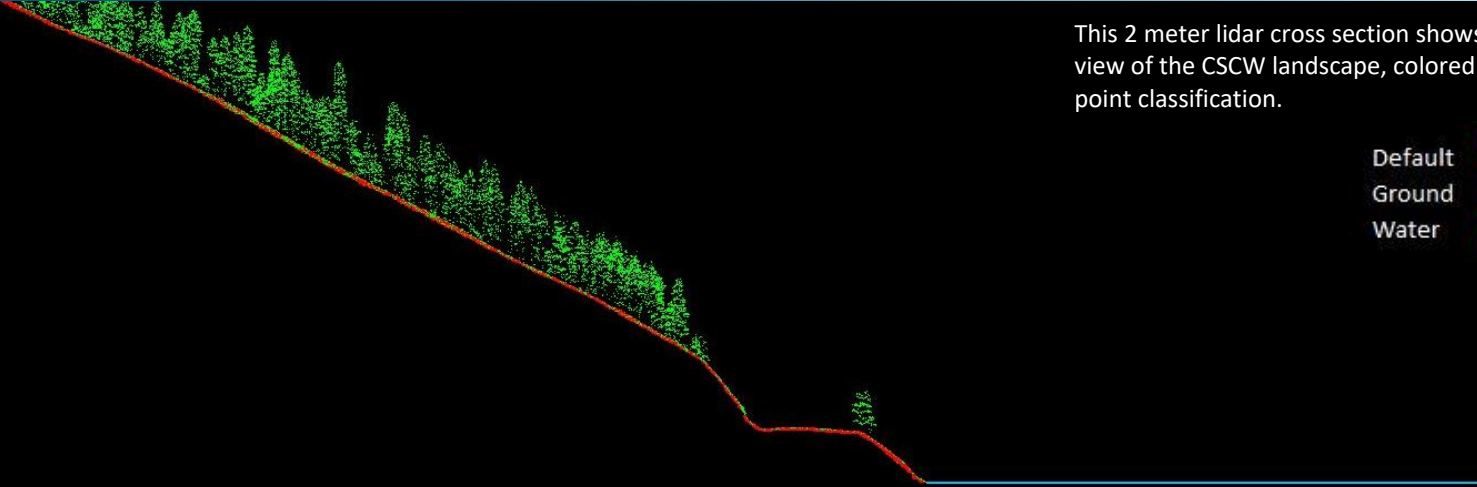


Figure 2: Ground survey location map

PROCESSING

This 2 meter lidar cross section shows a view of the CSCW landscape, colored by point classification.

Default
Ground
Water



Lidar Data

Upon completion of data acquisition, QSI processing staff initiated a suite of automated and manual techniques to process the data into the requested deliverables. Processing tasks included GPS control computations, smoothed best estimate trajectory (SBET) calculations, kinematic corrections, calculation of laser point position, sensor and data calibration for optimal relative and absolute accuracy, and lidar point classification (Table 8). Processing methodologies were tailored for the landscape. Brief descriptions of these tasks are shown in Table 9.

Table 8: ASPRS LAS classification standards applied to the CWCB Montrose dataset

Classification Number	Classification Name	Classification Description
1	Default/Unclassified	Laser returns that are not included in the ground class, composed of vegetation and anthropogenic features
1 - 0	Edge Clip / Overlap	Laser returns at the outer edges of flightlines that are geometrically unreliable
2	Ground	Laser returns that are determined to be ground using automated and manual cleaning algorithms
7 - W	Noise	Laser returns that are often associated with birds, scattering from reflective surfaces, or artificial points below the ground surface
9	Water	Laser returns that are determined to be water using automated and manual cleaning algorithms
17	Bridge	Bridge decks
18 -W	High Noise	Above-ground laser returns that are often associated with birds, scattering from reflective surfaces, or atmospheric noise

Classification Number	Classification Name	Classification Description
20	Ignored Ground	Ground points proximate to water's edge breaklines; ignored for correct model creation
21	Snow	Laser returns that are determined to be snow using automated and manual cleaning algorithms

Table 9: lidar processing workflow

Lidar Processing Step	Software Used
Resolve kinematic corrections for aircraft position data using kinematic aircraft GPS and static ground GPS data. Develop a smoothed best estimate of trajectory (SBET) file that blends post-processed aircraft position with sensor head position and attitude recorded throughout the survey.	POSPac MMS v.8.3
Calculate laser point position by associating SBET position to each laser point return time, scan angle, intensity, etc. Create raw laser point cloud data for the entire survey in *.las (ASPRS v. 1.4) format. Convert data to orthometric elevations by applying a geoid correction.	RiProcess v1.8.5
Import raw laser points into manageable blocks to perform manual relative accuracy calibration and filter erroneous points. Classify ground points for individual flight lines.	TerraScan v.19
Using ground classified points per each flight line, test the relative accuracy. Perform automated line-to-line calibrations for system attitude parameters (pitch, roll, heading), mirror flex (scale) and GPS/IMU drift. Calculate calibrations on ground classified points from paired flight lines and apply results to all points in a flight line. Use every flight line for relative accuracy calibration.	TerraMatch v.19
Classify resulting data to ground and other client designated ASPRS classifications (Table 8). Assess statistical absolute accuracy via direct comparisons of ground classified points to ground control survey data.	TerraScan v.19 TerraModeler v.19 LasMonkey 2.4.7 (QSI Proprietary)
Generate bare earth models as triangulated surfaces. Export all surface models as GeoTIFF format at a 1 meter pixel resolution.	LAS Product Creator 3.4 (QSI proprietary)
Generate contour lines from classified contour keypoints. Export all contours as polyline shapefiles in an ESRI Geodatabase.	TerraScan v.19 TerraModeler v.19 ArcMap v. 10.3.1

Feature Extraction

Hydroflattening and Water's Edge Breaklines

Water bodies within the project area were flattened to a consistent water level. Bodies of water that were flattened include lakes and other closed water bodies with a surface area greater than 2 acres, all streams and rivers that are nominally wider than 30 meters and select smaller bodies of water as feasible. The hydroflattening process eliminates artifacts in the digital terrain model caused by both increased variability in ranges or dropouts in laser returns due to the low reflectivity of water.

Hydroflattening of closed water bodies was performed through a combination of automated and manual detection and adjustment techniques designed to identify water boundaries and water levels. Boundary polygons were developed using an algorithm which weights lidar-derived slopes, intensities, and return densities to detect the water's edge. The water edges were then manually reviewed and edited as necessary.

Once polygons were developed the initial ground classified points falling within water polygons were reclassified as water points to omit them from the final ground model. Elevations were then obtained from the filtered lidar returns to create the final breaklines. Lakes were assigned a consistent elevation for an entire polygon while rivers were assigned consistent elevations on opposing banks and smoothed to ensure downstream flow through the entire river channel.

Special care was taken to flatten a series of dammed reservoirs which exist along a river within the AOI. Areas where the reservoir water level flattened out from the sloped river were deemed lakes. Temporal changes in water level corresponding to timing differences in reservoir dam releases and lidar collection dates caused the reservoir "lakes" to be flattened to their lowest collected water level so as to preserve as much valid topography as possible.

Water boundary breaklines were then incorporated into the hydroflattened DEM by enforcing triangle edges (adjacent to the breakline) to the elevation values of the breakline. This implementation corrected interpolation along the hard edge. Water surfaces were obtained from a TIN of the 3-D water edge breaklines resulting in the final hydroflattened model (Figure 3).

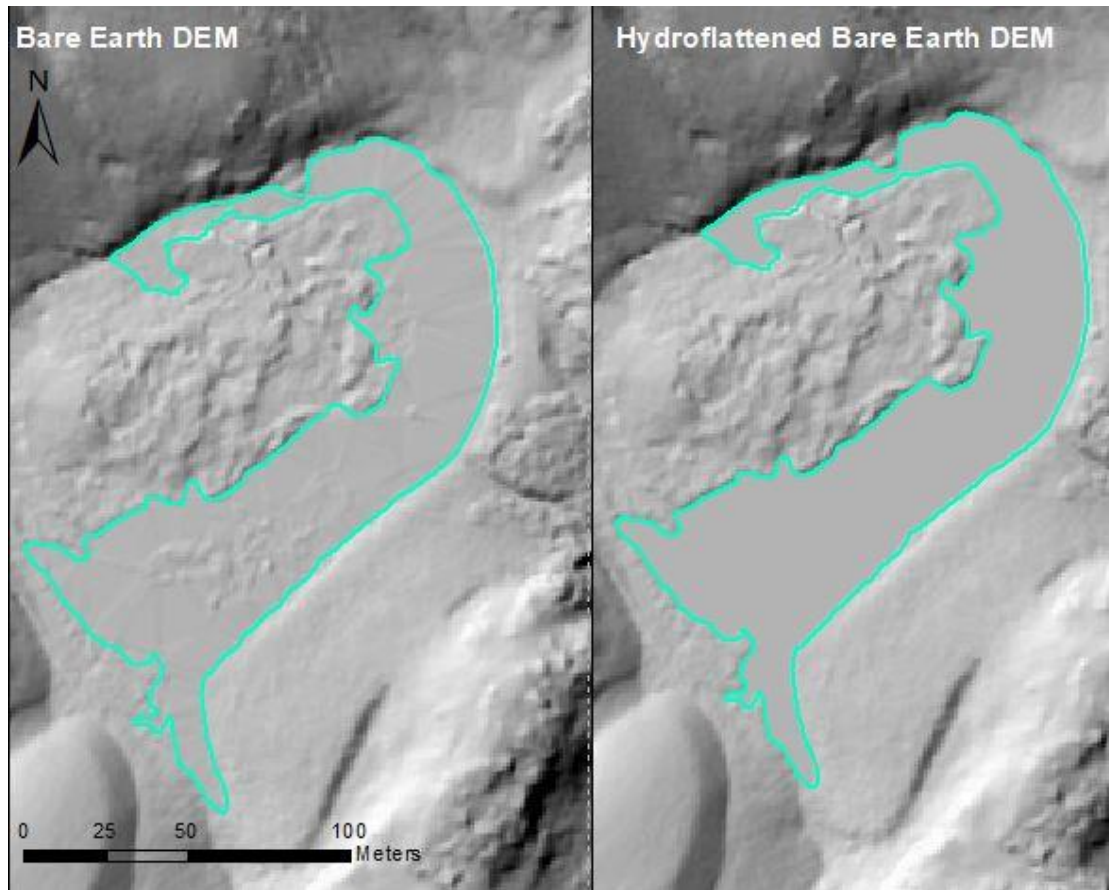
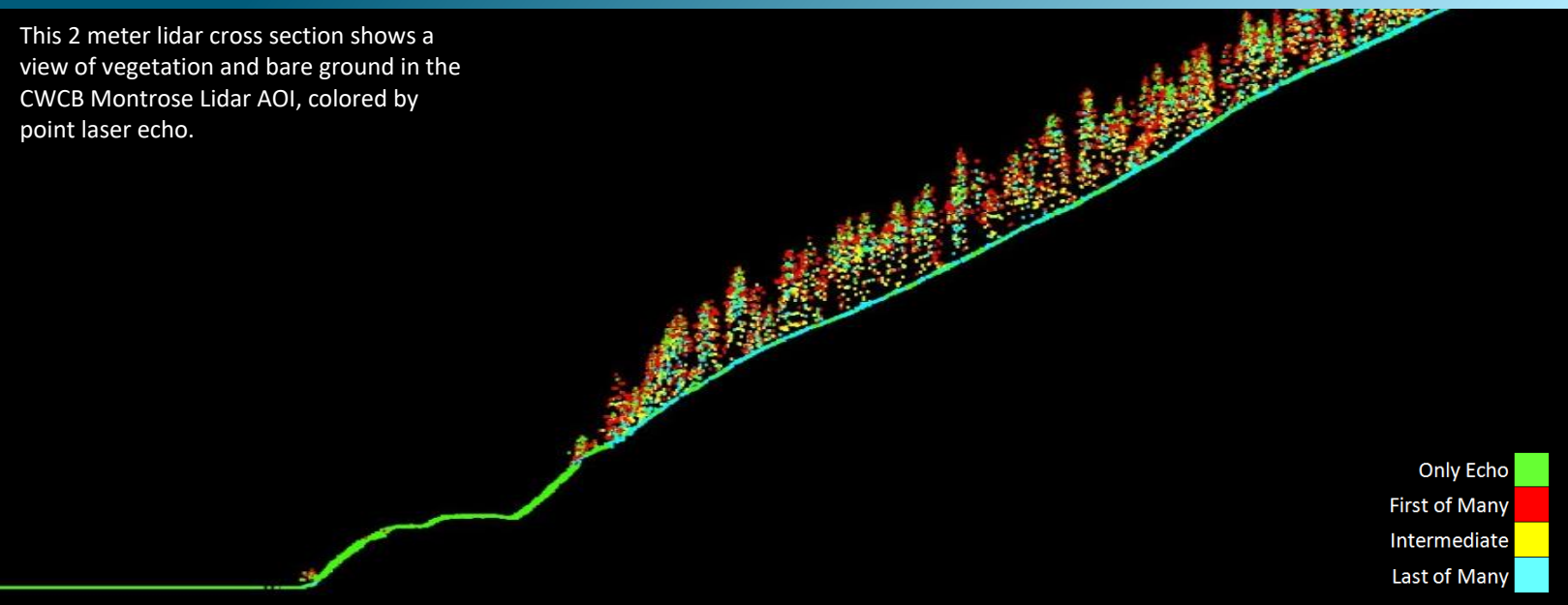


Figure 3: Example of hydroflattening in the CWCB Montrose Lidar dataset

Contours

Contour generation from lidar point data required a thinning operation in order to reduce contour sinuosity. The thinning operation reduced point density where topographic change is minimal (i.e., flat surfaces) while preserving resolution where topographic change was present. Model key points were selected from the ground model every 20 feet with the spacing decreased in regions with high surface curvature. Generation of model key points eliminated redundant detail in terrain representation, particularly in areas of low relief, and provided for a more manageable dataset. Contours were produced through TerraModeler by interpolating between the model key points at even elevation increments.

This 2 meter lidar cross section shows a view of vegetation and bare ground in the CWCB Montrose Lidar AOI, colored by point laser echo.



Lidar Density

The acquisition parameters were designed to acquire an average first-return density of 2 points/m². First return density describes the density of pulses emitted from the laser that return at least one echo to the system. Multiple returns from a single pulse were not considered in first return density analysis. Some types of surfaces (e.g., breaks in terrain, water and steep slopes) may have returned fewer pulses than originally emitted by the laser. First returns typically reflect off the highest feature on the landscape within the footprint of the pulse. In forested or urban areas the highest feature could be a tree, building or power line, while in areas of unobstructed ground, the first return will be the only echo and represents the bare earth surface.

The density of ground-classified lidar returns was also analyzed for this project. Terrain character, land cover, and ground surface reflectivity all influenced the density of ground surface returns. In vegetated areas, fewer pulses may penetrate the canopy, resulting in lower ground density.

The average first-return density of lidar data for the CWCB Montrose project was 6.25 points/m² while the average ground classified density was 2.32 points/m² (Table 10). The statistical and spatial distributions of first return densities and classified ground return densities per 100 m x 100 m cell are portrayed in Figure 4 through Figure 7.

Table 10: Average lidar point densities

Classification	Point Density
First-Return	6.25 points/m ²
Ground Classified	2.32 points/m ²

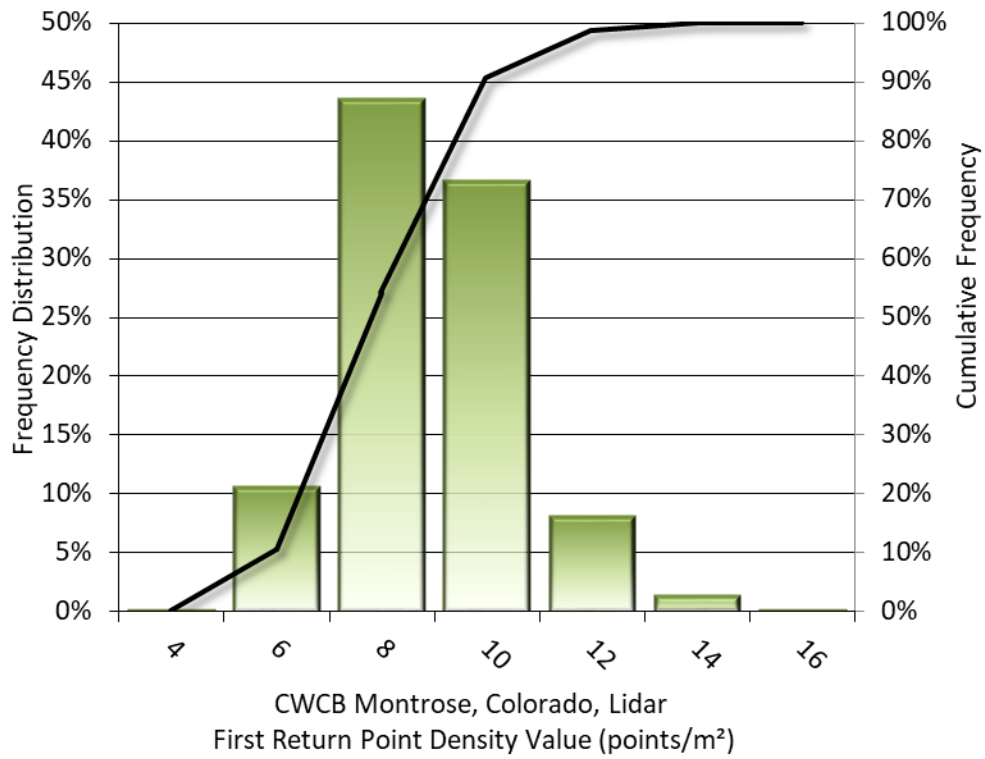


Figure 4: Frequency distribution of first return point density values per 100 x 100 m cell

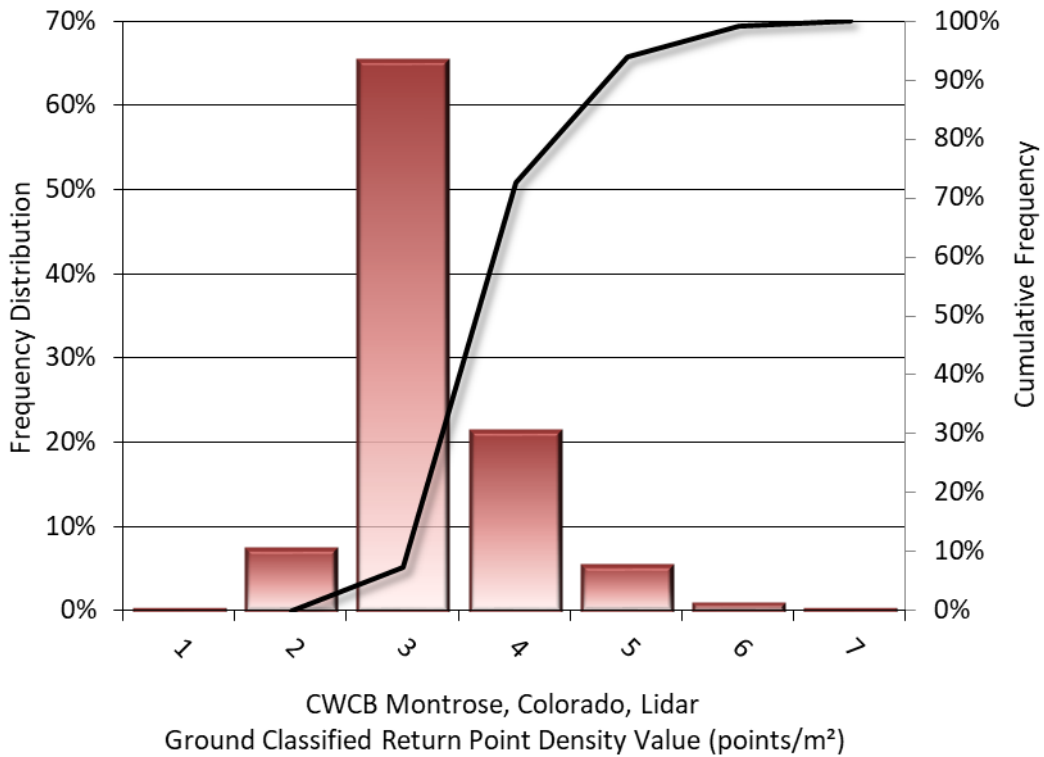


Figure 5: Frequency distribution of ground-classified return point density values per 100 x 100 m cell

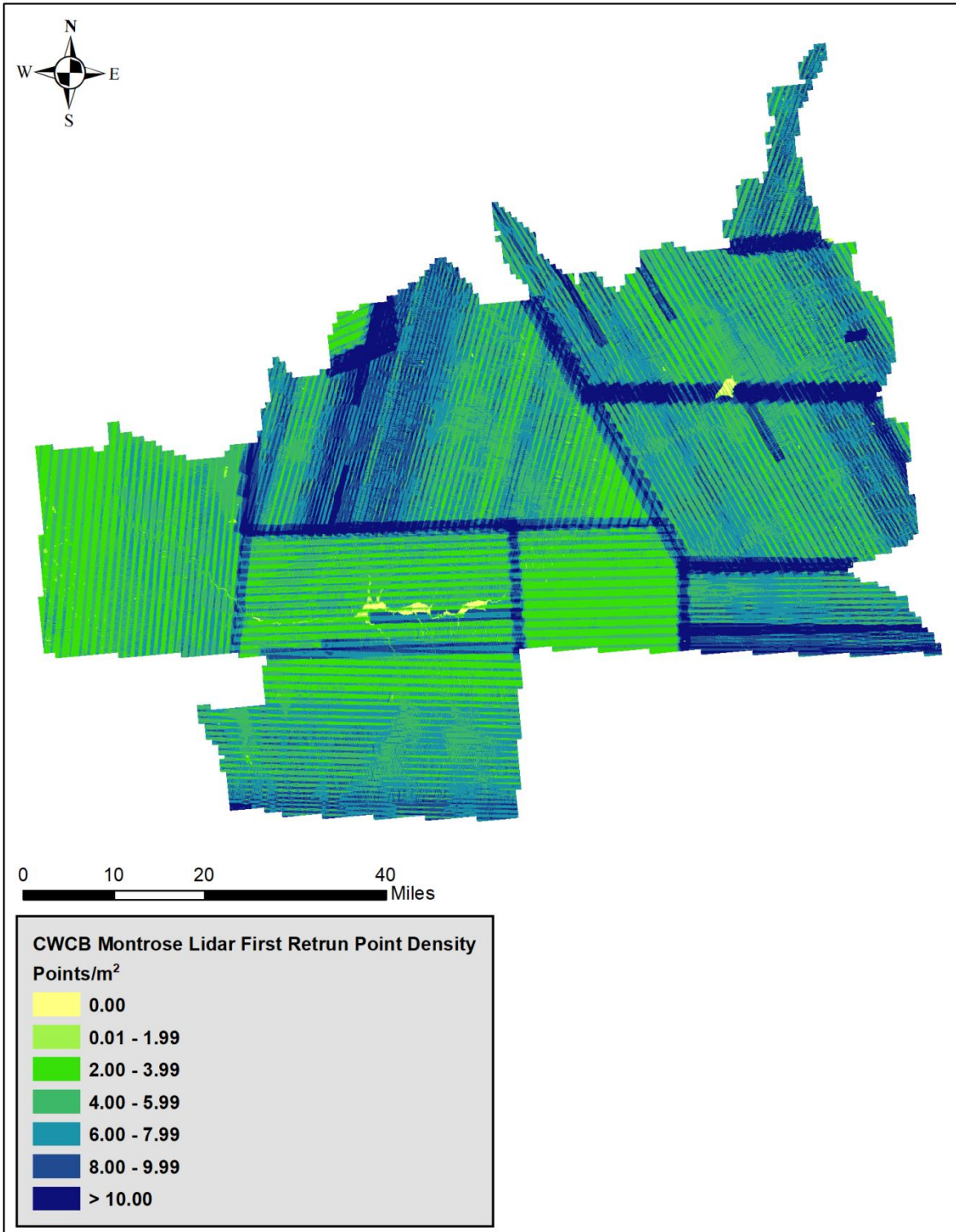


Figure 6: Native density map for the CWCB Montrose site (100 m x 100 m cells)

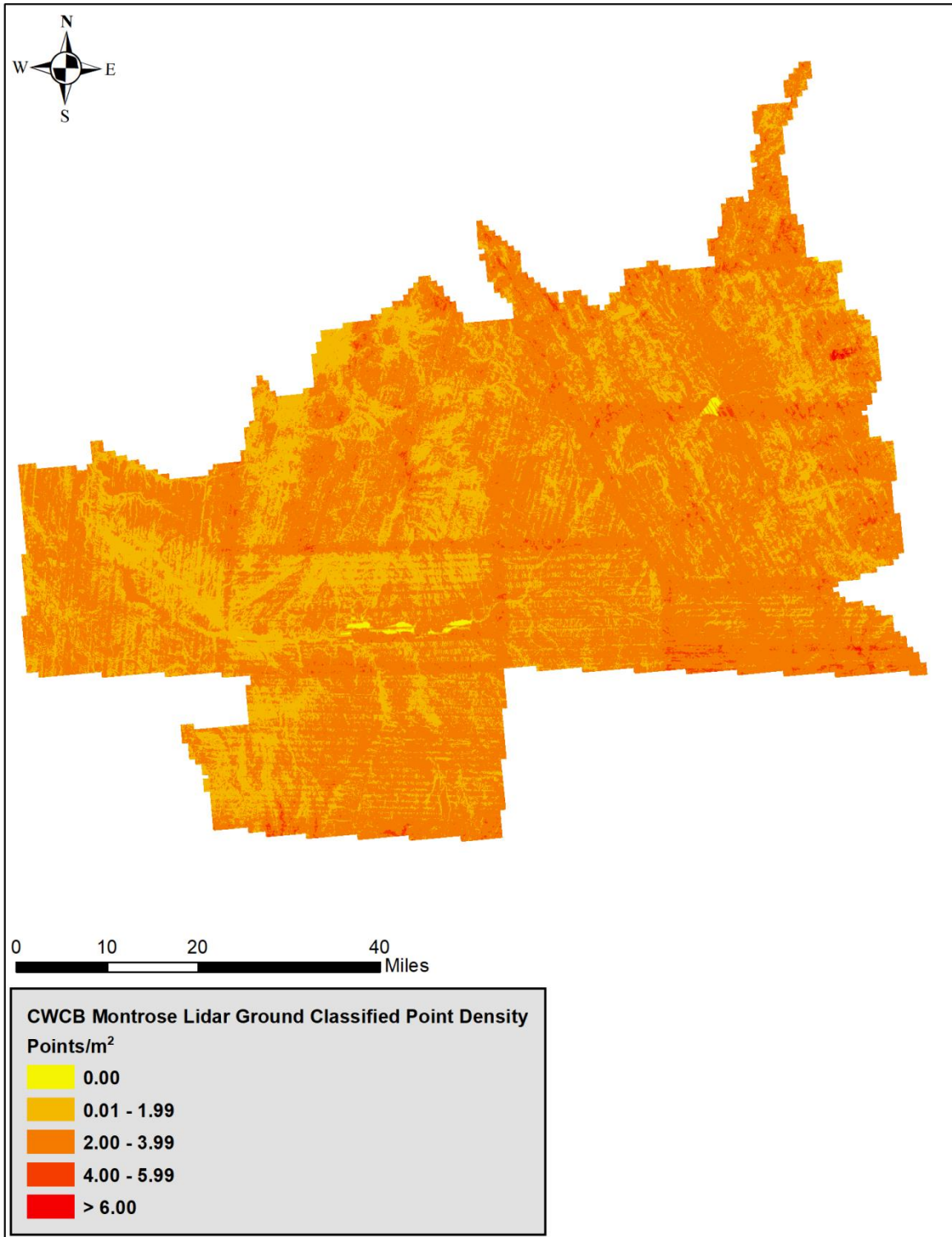


Figure 7: Ground point density map for the CWCB Montrose site (100 m x 100 m cells)

Lidar Accuracy Assessments

The accuracy of the lidar data collection can be described in terms of absolute accuracy (the consistency of the data with external data sources) and relative accuracy (the consistency of the dataset with itself). See Appendix A for further information on sources of error and operational measures used to improve relative accuracy.

Lidar Non-Vegetated Vertical Accuracy

Absolute accuracy was assessed using Non-Vegetated Vertical Accuracy (NVA) reporting designed to meet guidelines presented in the FGDC National Standard for Spatial Data Accuracy³. NVA compares known ground check point data that were withheld from the calibration and post-processing of the lidar point cloud to the triangulated surface generated by the unclassified lidar point cloud as well as the derived gridded bare earth DEM. NVA is a measure of the accuracy of lidar point data in open areas where the lidar system has a high probability of measuring the ground surface and is evaluated at the 95% confidence interval ($1.96 * RMSE$), as shown in Table 11.

The mean and standard deviation (sigma σ) of divergence of the ground surface model from quality assurance point coordinates are also considered during accuracy assessment. These statistics assume the error for x, y and z is normally distributed, and therefore the skew and kurtosis of distributions are also considered when evaluating error statistics. For the CWCB Montrose survey, 111 ground check points were withheld from the calibration and post processing of the lidar point cloud, with resulting non-vegetated vertical accuracy of 0.098 meters, as compared to unclassified LAS, and 0.098 meters as compared to the bare earth DEM, with 95% confidence (Figure 8, Figure 9).

QSI also assessed absolute accuracy using 134 ground control points. Although these points were used in the calibration and post-processing of the lidar point cloud, they still provide a good indication of the overall accuracy of the lidar dataset, and therefore have been provided in Table 11 and Figure 10.

³ Federal Geographic Data Committee, ASPRS POSITIONAL ACCURACY STANDARDS FOR DIGITAL GEOSPATIAL DATA EDITION 1, Version 1.0, NOVEMBER 2014.

https://www.asprs.org/a/society/committees/standards/Positional_Accuracy_Standards.pdf.

Table 11: Absolute accuracy results

Absolute Vertical Accuracy			
	NVA, as compared to unclassified LAS	NVA, as compared to bare earth DEM	Ground Control Points
Sample	111 points	111 points	134 points
95% Confidence (1.96*RMSE)	0.098 m	0.098 m	0.091 m
Average	-0.016 m	0.001 m	-0.004 m
Median	-0.015 m	-0.002 m	-0.003 m
RMSE	0.050 m	0.050 m	0.046 m
Standard Deviation (1σ)	0.048 m	0.050 m	0.046 m

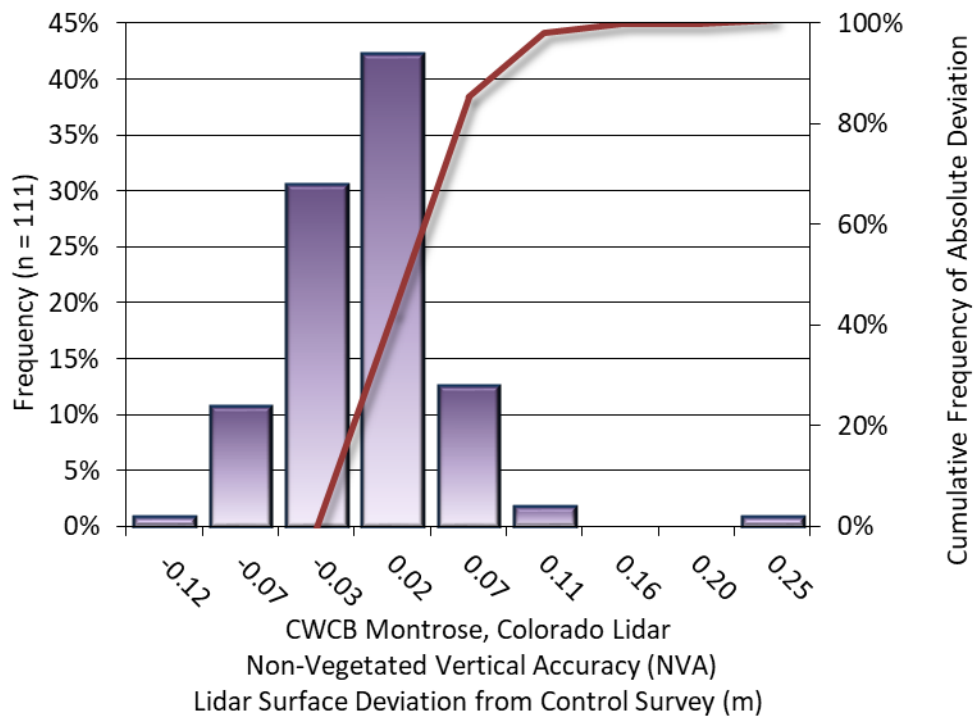


Figure 8: Frequency histogram for lidar unclassified LAS deviation from ground check point values (NVA)

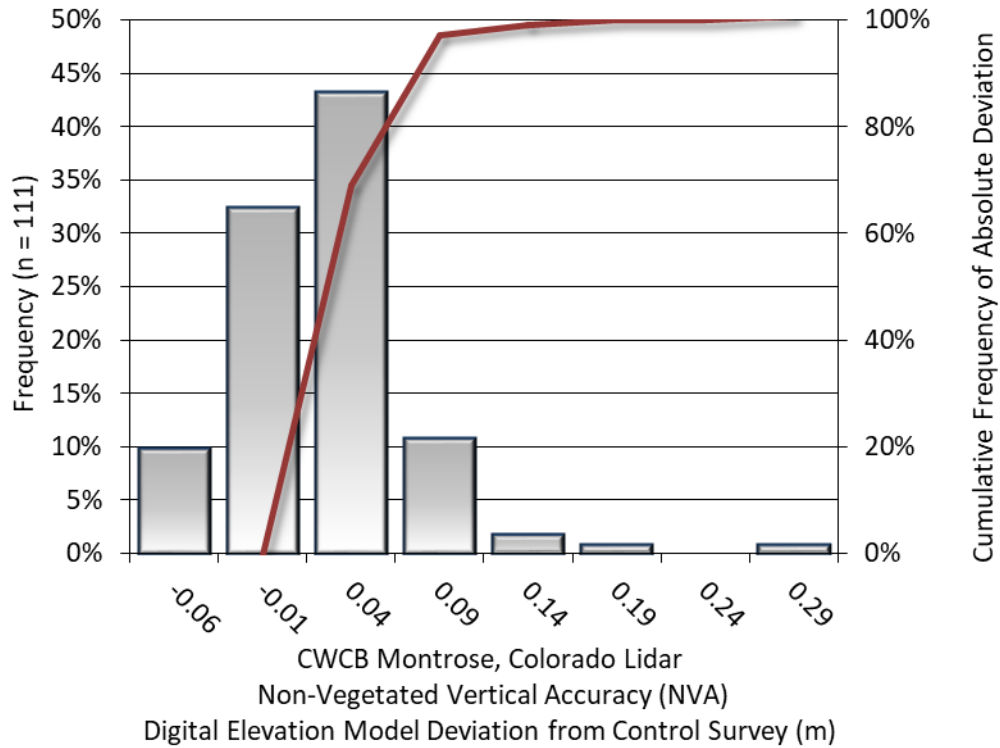


Figure 9: Frequency histogram for lidar bare earth DEM surface deviation from ground check point values (NVA)

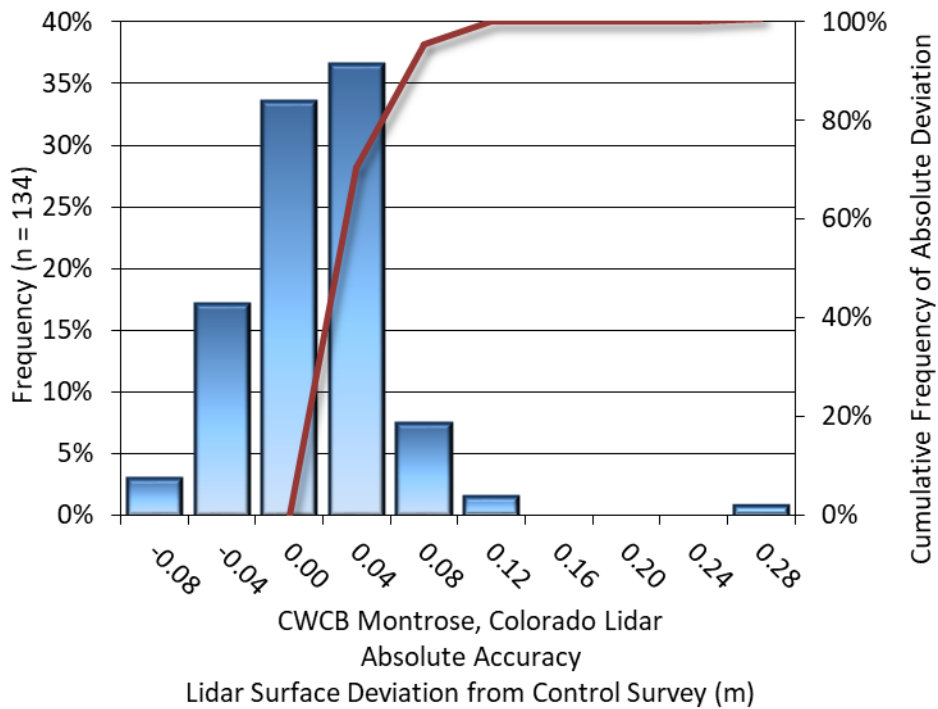


Figure 10: Frequency histogram for lidar surface deviation from ground control point values

Lidar Vegetated Vertical Accuracies

QSI also assessed vertical accuracy using Vegetated Vertical Accuracy (VVA) reporting. VVA compares known ground check point data collected over vegetated surfaces using land class descriptions to the triangulated ground surface generated by the ground classified lidar points. For the CWCB Montrose survey, 85 vegetated check points were collected, with resulting vegetated vertical accuracy of 0.287 meters as compared to the bare earth DEM, evaluated at the 95th percentile (Table 12, Figure 11).

Table 12: Vegetated vertical accuracy results

Vegetated Vertical Accuracy	
Sample	85 points
95 th Percentile	0.287 m
Average	-0.044 m
Median	-0.039 m
RMSE	0.140 m
Standard Deviation (1 σ)	0.134 m

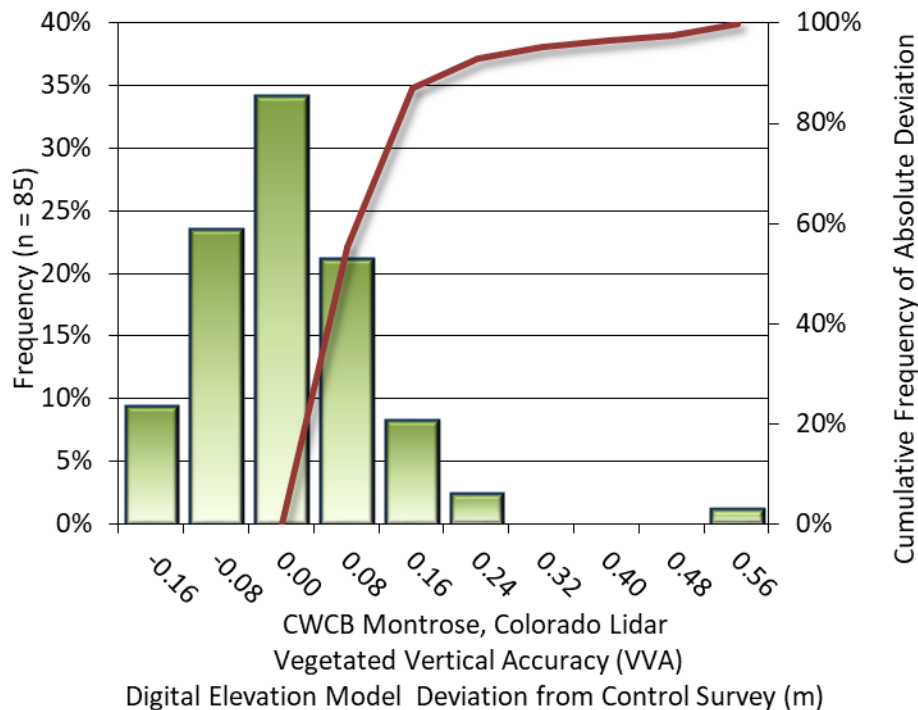


Figure 11: Frequency histogram for lidar surface deviation from vegetated check point values (VVA)

Lidar Relative Vertical Accuracy

Relative vertical accuracy refers to the internal consistency of the data set as a whole: the ability to place an object in the same location given multiple flight lines, GPS conditions, and aircraft attitudes. When the lidar system is well calibrated, the swath-to-swath vertical divergence is low (<0.10 meters). The relative vertical accuracy was computed by comparing the ground surface model of each individual flight line with its neighbors in overlapping regions. The average (mean) line to line relative vertical accuracy for the CWCB Montrose Lidar project was 0.052 meters (Table 13, Figure 12).

Table 13: Relative accuracy results

Relative Accuracy	
Sample	314 flight line surfaces
Average	0.052 m
Median	0.053 m
RMSE	0.054 m
Standard Deviation (1σ)	0.009 m
1.96 σ	0.017 m

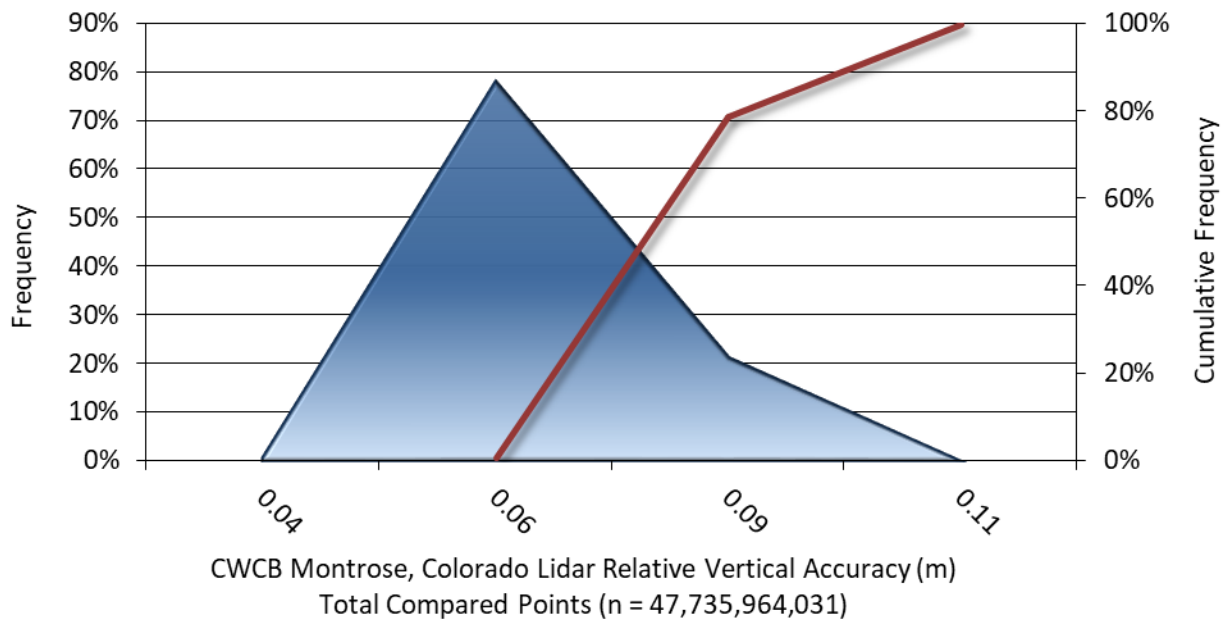


Figure 12: Frequency plot for relative vertical accuracy between flight lines

Lidar Horizontal Accuracy

Lidar horizontal accuracy is a function of Global Navigation Satellite System (GNSS) derived positional error, flying altitude, and INS derived attitude error. The obtained RMSE_r value is multiplied by a conversion factor of 1.7308 to yield the horizontal component of the National Standards for Spatial Data Accuracy (NSSDA) reporting standard where a theoretical point will fall within the obtained radius 95 percent of the time. Based on a flying altitude of 1,159 meters, an IMU error of 0.010 decimal degrees, and a GNSS positional error of 0.015 meters, this project was compiled to meet 0.015 m horizontal accuracy at the 95% confidence level (Table 14).

Table 14: Horizontal Accuracy

Horizontal Accuracy	
RMSE _r	0.00 m
ACC _r	0.01 m

CERTIFICATIONS

Quantum Spatial, Inc. provided lidar services for the CWCB Montrose project as described in this report.

I, John English, have reviewed the attached report for completeness and hereby state that it is a complete and accurate report of this project.

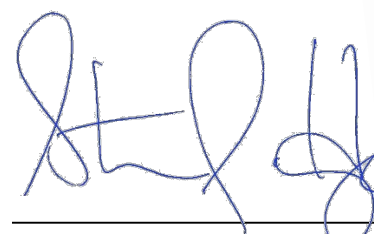
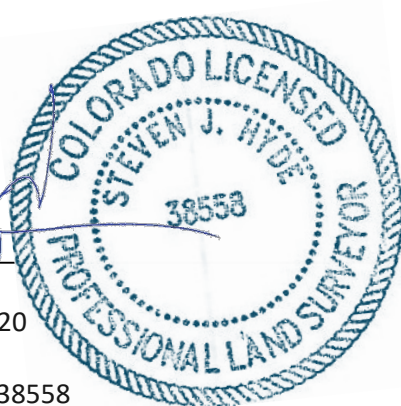
John T. English

Jul 17, 2020

John English
Project Manager
Quantum Spatial, Inc.

I, Steven J. Hyde, PLS, being duly registered as a Professional Land Surveyor in and by the state of Colorado, hereby certify that the methodologies, static GNSS occupations used during airborne flights, and ground survey point collection were performed using commonly accepted Standard Practices. Field work for this report was conducted between August 21, 2019 and September 24, 2019.

Accuracy statistics shown in the Accuracy Section of this Report have been reviewed by me and found to meet the "National Standard for Spatial Data Accuracy".

Steven J. Hyde, PLS 07/17/2020
Quantum Spatial, Inc.
Colorado Licensed Surveyor # 38558

1-sigma (σ) Absolute Deviation: Value for which the data are within one standard deviation (approximately 68th percentile) of a normally distributed data set.

1.96 * RMSE Absolute Deviation: Value for which the data are within two standard deviations (approximately 95th percentile) of a normally distributed data set, based on the FGDC standards for Non-vegetated Vertical Accuracy (NVA) reporting.

Accuracy: The statistical comparison between known (surveyed) points and laser points. Typically measured as the standard deviation (σ) and root mean square error (RMSE).

Absolute Accuracy: The vertical accuracy of lidar data is described as the mean and standard deviation (σ) of divergence of lidar point coordinates from ground survey point coordinates. To provide a sense of the model predictive power of the dataset, the root mean square error (RMSE) for vertical accuracy is also provided. These statistics assume the error distributions for x, y and z are normally distributed, and thus we also consider the skew and kurtosis of distributions when evaluating error statistics.

Relative Accuracy: Relative accuracy refers to the internal consistency of the data set; i.e., the ability to place a laser point in the same location over multiple flight lines, GPS conditions and aircraft attitudes. Affected by system attitude offsets, scale and GPS/IMU drift, internal consistency is measured as the divergence between points from different flight lines within an overlapping area. Divergence is most apparent when flight lines are opposing. When the lidar system is well calibrated, the line-to-line divergence is low (<10 cm).

Root Mean Square Error (RMSE): A statistic used to approximate the difference between real-world points and the lidar points. It is calculated by squaring all the values, then taking the average of the squares and taking the square root of the average.

Data Density: A common measure of lidar resolution, measured as points per square meter.

Digital Elevation Model (DEM): File or database made from surveyed points, containing elevation points over a contiguous area. Digital terrain models (DTM) and digital surface models (DSM) are types of DEMs. DTMs consist solely of the bare earth surface (ground points), while DSMs include information about all surfaces, including vegetation and man-made structures.

Intensity Values: The peak power ratio of the laser return to the emitted laser, calculated as a function of surface reflectivity.

Nadir: A single point or locus of points on the surface of the earth directly below a sensor as it progresses along its flight line.

Overlap: The area shared between flight lines, typically measured in percent. 100% overlap is essential to ensure complete coverage and reduce laser shadows.

Pulse Rate (PR): The rate at which laser pulses are emitted from the sensor; typically measured in thousands of pulses per second (kHz).

Pulse Returns: For every laser pulse emitted, the number of wave forms (i.e., echoes) reflected back to the sensor. Portions of the wave form that return first are the highest element in multi-tiered surfaces such as vegetation. Portions of the wave form that return last are the lowest element in multi-tiered surfaces.

Real-Time Kinematic (RTK) Survey: A type of surveying conducted with a GPS base station deployed over a known monument with a radio connection to a GPS rover. Both the base station and rover receive differential GPS data and the baseline correction is solved between the two. This type of ground survey is accurate to 1.5 cm or less.

Post-Processed Kinematic (PPK) Survey: GPS surveying is conducted with a GPS rover collecting concurrently with a GPS base station set up over a known monument. Differential corrections and precisions for the GNSS baselines are computed and applied after the fact during processing. This type of ground survey is accurate to 1.5 cm or less.

Scan Angle: The angle from nadir to the edge of the scan, measured in degrees. Laser point accuracy typically decreases as scan angles increase.

Native Lidar Density: The number of pulses emitted by the lidar system, commonly expressed as pulses per square meter.

APPENDIX A - ACCURACY CONTROLS

Relative Accuracy Calibration Methodology:

Manual System Calibration: Calibration procedures for each mission require solving geometric relationships that relate measured swath-to-swath deviations to misalignments of system attitude parameters. Corrected scale, pitch, roll and heading offsets were calculated and applied to resolve misalignments. The raw divergence between lines was computed after the manual calibration was completed and reported for each survey area.

Automated Attitude Calibration: All data were tested and calibrated using TerraMatch automated sampling routines. Ground points were classified for each individual flight line and used for line-to-line testing. System misalignment offsets (pitch, roll and heading) and scale were solved for each individual mission and applied to respective mission datasets. The data from each mission were then blended when imported together to form the entire area of interest.

Automated Z Calibration: Ground points per line were used to calculate the vertical divergence between lines caused by vertical GPS drift. Automated Z calibration was the final step employed for relative accuracy calibration.

Lidar accuracy error sources and solutions:

Type of Error	Source	Post Processing Solution
GPS (Static/Kinematic)	Long Base Lines	None
	Poor Satellite Constellation	None
	Poor Antenna Visibility	Reduce Visibility Mask
Relative Accuracy	Poor System Calibration	Recalibrate IMU and sensor offsets/settings
	Inaccurate System	None
Laser Noise	Poor Laser Timing	None
	Poor Laser Reception	None
	Poor Laser Power	None
	Irregular Laser Shape	None

Operational measures taken to improve relative accuracy:

Low Flight Altitude: Terrain following was employed to maintain a constant above ground level (AGL). Laser horizontal errors are a function of flight altitude above ground (about 1/3000th AGL flight altitude).

Focus Laser Power at narrow beam footprint: A laser return must be received by the system above a power threshold to accurately record a measurement. The strength of the laser return (i.e., intensity) is a function of laser emission power, laser footprint, flight altitude and the reflectivity of the target. While surface reflectivity cannot be controlled, laser power can be increased and low flight altitudes can be maintained.

Reduced Scan Angle: Edge-of-scan data can become inaccurate. The scan angle was reduced to a maximum of $\pm 29.25^\circ$ from nadir, creating a narrow swath width and greatly reducing laser shadows from trees and buildings.

Quality GPS: Flights took place during optimal GPS conditions (e.g., 6 or more satellites and PDOP [Position Dilution of Precision] less than 3.0). Before each flight, the PDOP was determined for the survey day. During all flight times, a dual frequency DGPS base station recording at 1 second epochs was utilized and a maximum baseline length between the aircraft and the control points was less than 13 nm at all times.

Ground Survey: Ground survey point accuracy (<1.5 cm RMSE) occurs during optimal PDOP ranges and targets a minimal baseline distance of 4 miles between GPS rover and base. Robust statistics are, in part, a function of sample size (n) and distribution. Ground survey points are distributed to the extent possible throughout multiple flight lines and across the survey area.

50% Side-Lap (100% Overlap): Overlapping areas are optimized for relative accuracy testing. Laser shadowing is minimized to help increase target acquisition from multiple scan angles. Ideally, with a 50% side-lap, the nadir portion of one flight line coincides with the swath edge portion of overlapping flight lines. A minimum of 50% side-lap with terrain-followed acquisition prevents data gaps.

Opposing Flight Lines: All overlapping flight lines have opposing directions. Pitch, roll and heading errors are amplified by a factor of two relative to the adjacent flight line(s), making misalignments easier to detect and resolve.